Dielectric measurements with an open-ended coaxial probe

T.P. Marsland, MA, PhD
S. Evans, MA, PhD

Indexing terms: Dielectric materials, Permittivity, Antennas (measurements), Coaxial components

Abstract: The paper is concerned with the use of an open-ended coaxial-line probe for making dielectric measurements on lossy materials. The input reflection coefficient of the probe is measured with a network analyser, and the permittivity is determined using an approximate circuit model for the probe admittance. Applying the cross-ratio invariance property of the bilinear transform to two such circuit models, we derive a simplified procedure that permits simultaneous calibration of the probe and error correction of the network analyser. Estimates of the resulting uncertainties are given, and the technique is illustrated with experimental measurements on known dielectric liquids between 50 MHz and 2.6 GHz.

1 Introduction

Radio-frequency or microwave power is sometimes the most appropriate for the controlled heating of materials in both industrial and medical applications [1, 2], and measurements of the material dielectric properties are crucial to the design of systems which use such techniques. Since the application is to heating, it is likely that measurements must cover a range of temperatures different from the ambient temperature, and it is likely that the material will be lossy. Furthermore, one will need to know the material properties over a wide frequency range as part of the initial design considerations. There is a range of dielectric measurement techniques available in the literature [3], however the open-ended coaxial probe is particularly suitable for meeting these needs: it can cover a wide range of tan δ, it is convenient for insertion into a temperature-controlled environment, and a given size of probe can cover a two-decade frequency range. There is also the general convenience that little or no sample preparation is necessary: if solid, the probe is merely pushed into contact with the material to be measured.

Our particular interest is in measuring the dielectric properties of cryopreserved tissue, with the aim of surveying a wide range of temperatures and frequencies to permit more successful rewarming of organs than that previously achieved [4]. Experimental results on both perfused tissue and perfusate solutions relevant to this work are presented elsewhere [5]. We have used a probe made from a length of 6.4 mm diameter semirigid coaxial cable, and measurement of the admittance presented at the end in contact with the unknown material allows the determination of the permittivity and conductivity.

Electrically short antennas were first used for the measurement of permittivity and permeability towards the end of the 1950s [6], however, Tanabe and Joines [7] introduced the open-ended coaxial-probe technique. Burdette *et al.* [8] developed the technique further and made many measurements of the dielectric properties of various tissues; including cryopreserved organs over a range of temperatures, and Stuchly and Stuchly [9] have investigated the open-ended probe in detail, both theoretically and experimentally.

2 Probe geometry

The probes we have used were constructed from standard 6.4 mm diameter 50 Ω Teflon-filled semirigid coaxial cable (RG401) whose dimensions are shown in Fig. 1*a*.

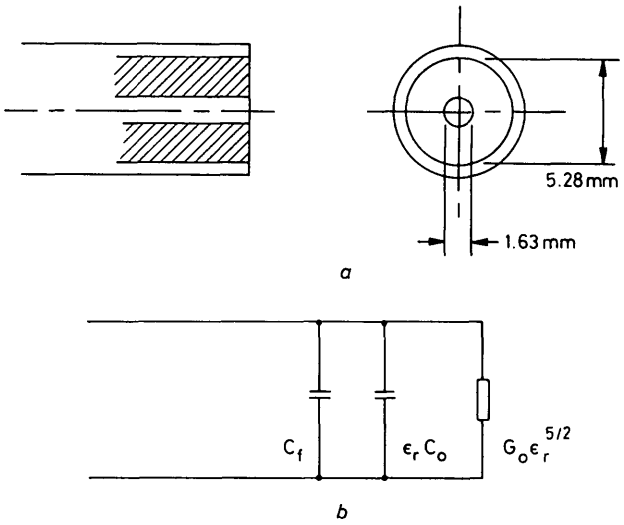

Fig. 1 *Open-ended coaxial probe*

a Geometry and dimensions of open-ended coaxial probe. The probe is made from RG401 semirigid cable, and the end shown below is gold plated to reduce corrosion

b Approximate equivalent circuit model of probe

Each probe was made from 300 mm lengths of heat-treated RG401 cable; one end was faced off flat and gold plated to prevent corrosion, the other was attached to a standard male Type-N connector. The choice of probe dimensions is necessarily a compromise between the lowest frequency at which useful measurements can be

Paper 5438H (E12, S2), first received 10th October 1986 and in revised form 26th March 1987

Dr. Evans is, and Dr. Marsland was formerly, with Cambridge University Engineering Department, Trumpington Street, Cambridge CB2 1PZ, United Kingdom. Dr. Marsland is now with MRC Medical Cryobiology Group, University Department of Surgery, Douglas House, Trumpington Road, Cambridge CB2 2AH, United Kingdom

made and the volume interrogated by the probe. This diameter cable allows us to go down to about 50 MHz with sample volumes of about 20 ml for lossy materials.

3 Electromagnetic fields of the open-ended probe

The electromagnetic field at the probe aperture is that of an ideal TEM guide with other field components which form the fringing field superimposed to satisfy the boundary conditions at the open end. Because of the axial symmetry, only TM_{0M} modes are excited by the discontinuity, thus the aperture field can be represented as the summation of the TEM mode and a series of TM_{0M} modes. Mosig *et al.* [10] used this modal representation to calculate the reflection coefficient of the TEM mode for a range of dielectric permittivities, the results were presented as a nomogram for each frequency.

Unfortunately this exact analysis is rather involved, and calculating the dielectric permittivity from measured data would require considerable computational effort since a closed form expression for the field is not available. Consequently, most workers have used an approximate equivalent circuit model for this sensor to provide a simpler, if less accurate, way to determine the permittivity from the probe input admittance.

4 Equivalent circuit models

In RG401 semirigid coaxial cable, the lowest TM mode, TM_{01}, has a cut-off frequency of about 56 GHz. At the frequencies where the probe is used for dielectric measurement, the effect of the discontinuity extends only a few millimetres into the guide, e.g. below 10 GHz, TM_{01} is attenuated by about 14 dB/mm. Thus the probe can be modelled by lumped circuit elements located at the end of an ideal open-circuited line. Burdette *et al.* [8] considered a general probe geometry and used an antenna modelling theorem due to Deschamps [11] to relate the impedance of the probe to the dielectric permittivity. A derivation specifically for the open-ended probe has been given by Brady *et al.* [12] which is outlined below. Fig. 1*a* shows the geometry.

In a nonmagnetic medium ($\mu_r = 1$), the Deschamps modelling theorem can be written

$$Y(\omega, \varepsilon_r \varepsilon_0) = \sqrt{\varepsilon_r}\, Y(\omega\sqrt{\varepsilon_r}, \varepsilon_0) \tag{1}$$

where Y is the antenna admittance, ε_r is the relative permittivity (possibly complex) of the material in which the antenna is embedded, and ε_0 and ω have their usual significance. The theorem applies to any probe geometry provided the medium that surrounds it is infinite in extent, in other words the radiation field must be wholly contained in the medium. Marcuvitz [13] gives an analytic expression for the equivalent circuit admittance of a coaxial aperture radiating into free space. At frequencies where the dimensions are small compared with the wavelength, this can be written

$$Y_a(\omega, \varepsilon_0) = a_4 \omega^4 + j a_1 \omega \tag{2}$$

where a_1 and a_4 are functions of the geometry only. Applying eqn. 1 to eqn. 2 gives

$$Y(\omega, \varepsilon_r \varepsilon_0) = G_0(\omega)\varepsilon_r^{5/2} + j\omega C_0 \varepsilon_r \tag{3}$$

where $G_0(\omega)$ is the free-space radiation conductance, and C_0 is the capacitance that represents the fringing field. Note that G_0 is predicted to vary as ω^4, but we shall not need to assume this functional relation. However, eqn. 3 is not strictly valid, for the following reasons:

a The field at the feed point of the probe (the aperture) is not purely TEM, therefore there is no unique admittance and eqn. 1 cannot be applied [6, 11].

b Marcuvitz's original derivation is only approximate since the aperture field is assumed to be purely TEM.

c Eqn. 2 is derived for a coaxial aperture in an infinite ground plane whereas the open-ended probe possesses a very small ground plane (the thickness of the outer).

Calculations performed by Bahl and Stuchly [14] suggest that absence of the infinite ground plane has little effect. Brady *et al.* attempt to resolve the remaining difficulties by assuming the equivalent circuit capacitance can be decomposed into two separate terms. A capacitance C_f represents the fringing field in the Teflon dielectric of the cable, and another parallel capacitance $\varepsilon_r C_0$ represents the fringing field in the external dielectric material, usually $C_0 \gg C_f$. This equivalent circuit model is shown in Fig. 1*b*. The admittance of the probe, normalised to the TEM characteristic impedance Z_0, is

$$y(\omega, \varepsilon_r) = G_0 Z_0 \varepsilon_r^{5/2} + j\omega Z_0(\varepsilon_r C_0 + C_f) \tag{4}$$

which we refer to as admittance model I.

From the explicit expressions for a_4 and a_1 [13] it can be shown that $G_0 \ll \omega C_0$ for coaxial lines that are small compared with the wavelength, suggesting a further simplification, used by several workers [15, 16, 17], which is to neglect G_0 altogether. With this simplification, eqn. 4 becomes

$$y(\omega, \varepsilon_r) = j\omega Z_0(\varepsilon_r C_0 + C_f) \tag{5}$$

which we refer to as admittance model II. In a later paper, Stuchly *et al.* [18] examine this simplification more carefully and suggest that it can lead to errors at high frequencies for large permittivities. In fact the fringing capacitance and the radiation conductance will be functions of the permittivity of the material being measured, although this variation is neglected in this work.

5 Field penetration

The analysis above assumes that the dielectric material is semi-infinite in extent. In practice, the probe must be presented with a sample of finite thickness, and so it is important to establish how far the field penetrates in a particular dielectric medium. Although this can be done theoretically (see, e.g. Reference 19) or experimentally for measurements on dielectric liquids, it is more difficult for biological materials because of their inhomogeneity.

The particular field distribution present (and hence the equivalent circuit parameters) depend on the surface conditions at the probe tip. Thus it is important to ensure the probe is cleaned after each measurement and, for semisolid materials, to ensure constant contact pressure between the probe and the material.

6 Microwave measurement of one-port networks

To measure the permittivity of an unknown dielectric material, the input reflection coefficient of the probe must be measured, whatever the circuit model. We have made measurements with such probes using both time-domain and frequency-domain network analysers; we concentrate here on the frequency-domain instrumentation.

The network-analyser system we have used consists of a Hewlett-Packard 8754A opt H26 network analyser and an 8502A test set. This configuration is capable of measuring the reflection coefficient of the probe in magnitude

and phase over a 50 MHz to 2.6 GHz frequency range. Fig. 2 shows a block diagram of the system. A microcomputer-controlled interface of our own design records measurements using a 12-bit analogue-to-digital convertor (ADC). The network-analyser source is controlled by a 12-bit digital-to-analogue convertor (DAC);

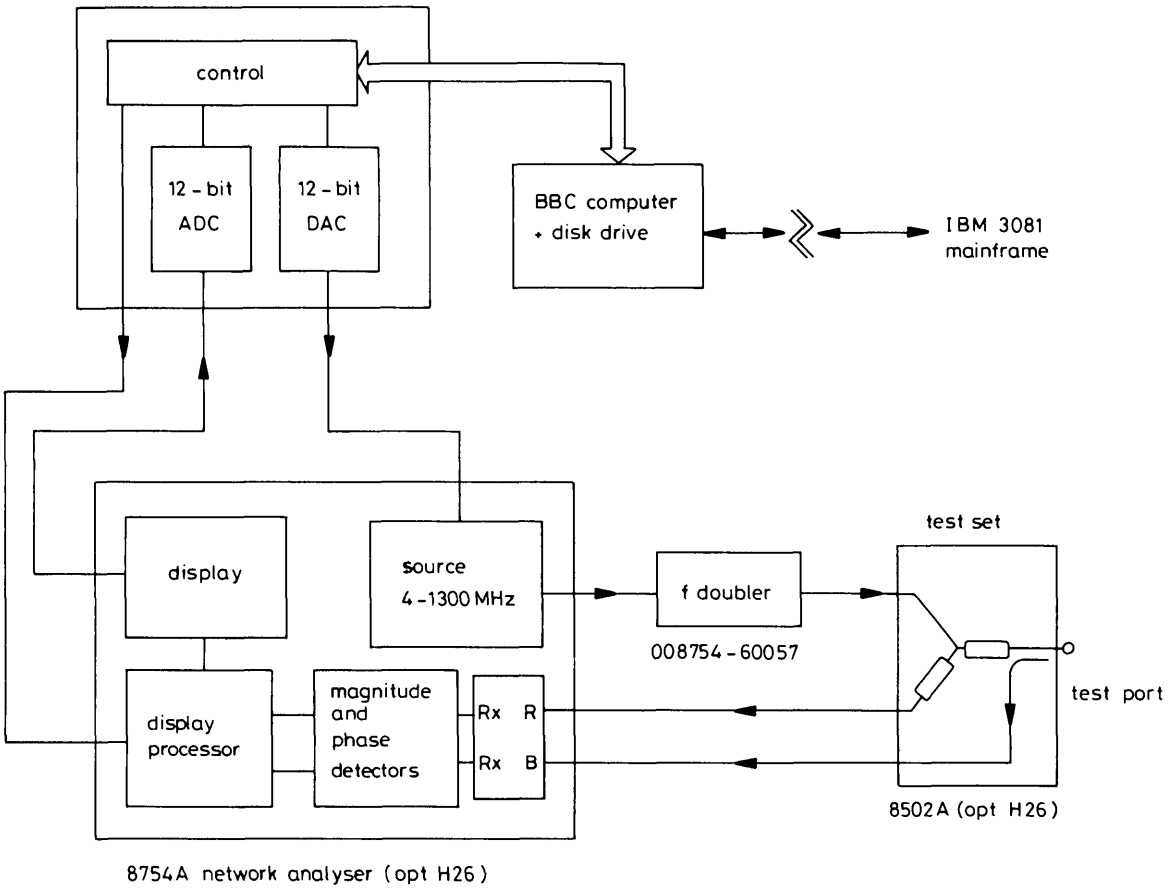

Fig. 2 *Block diagram of HP8754A network analyser. HP8502A test set and microcomputer-controlled data recorder*
After an experimental run has been completed, the data are transferred via a serial link to an IBM3081 mainframe computer

the sampled data are averaged and stored at each of 512 discrete frequencies. At the end of the sweep, the data are recorded on floppy disk, and at the end of a complete experimental run, the data are transmitted to an IBM 3081 mainframe computer for processing. Typically, 128 samples were averaged at each frequency, taking a total of 25 seconds to record both magnitude and phase at 512 discrete frequencies [20].

There are a number of imperfections inherent in any real network-analyser system: in the test set, cabling and connectors. It is conventional to model this imperfect network analyser measuring a one-port network as a perfect network analyser connected to the one-port network via a two-port embedding network with scattering matrix **E**.

If the admittance is to be measured accurately, the effects of the embedding network must be removed. The true reflection coefficient Γ_m can be calculated from a measured value ρ_m using the bilinear transform

$$\Gamma_m = \frac{\rho_m - E_{11}}{\rho_m E_{22} - (E_{11}E_{22} - E_{12}E_{21})} \quad (6)$$

We show in the following Sections how this separate step, and the need to find **E**, can be avoided altogether when making admittance measurements.

7 Error correction and probe calibration

Conventional network-analyser calibration procedures use measurements of three (or more) known terminations, e.g. short, open and match at each measurement frequency to determine the necessary elements of **E**. The problem here is that the known terminations must be applied at the probe tip. A close approach to the short circuit condition can be provided by pressing several layers of metal foil against the end of the probe. The open-circuit condition can be realised (very approximately) by leaving the probe open into air, however, the provision of a matched load is much more difficult. Such a component would be expensive to manufacture and extremely difficult to design so that it was both repeatable and had an accurately known reflection coefficient.

Kraszewski *et al.* [21], recognising these difficulties, suggested the use of polar liquids of known dielectric properties as terminations for the probe. Then, provided the equivalent circuit parameters of the probe are known, the elements of **E** can be determined from a simple set of expressions. The circuit parameters can be estimated from the probe geometry, but the fields at the probe tip are dependent on the surface finish, also the conductors in real semirigid cable are not accurately coaxial, and so an experimental technique is preferable here.

The error correction procedures described above split the work into two stages: (i) determine **E**, and (ii) use it to correct errors in subsequent measurements. Notice that step (i) is auxiliary; in that **E** is needed only for error correction. In fact, the need to calculate **E** can be eliminated altogether. By substituting three known admit-

tances $\{y_1, y_2, y_3\}$ together with corresponding reflection-coefficient measurements $\{\rho_1, \rho_2, \rho_3\}$ successively into eqn. 6 and eliminating the terms of **E** between them, we obtain a simple expression for the admittance y_m corresponding to a measured ρ_m:

$$y_m = -\frac{\Delta_{m1}\Delta_{32}\,y_3\,y_2 + \Delta_{m2}\,\Delta_{13}\,y_1 y_3 + \Delta_{m3}\,\Delta_{21} y_2\,y_1}{\Delta_{m1}\Delta_{32}\,y_1 + \Delta_{m2}\,\Delta_{13}\,y_2 + \Delta_{m3}\,\Delta_{21} y_3} \quad (7)$$

where $\Delta_{ij} = \rho_i - \rho_j$. This quite general result follows from the cross-ratio invariance property of the bilinear transform [22, 23]. There is a bilinear relationship both between the admittances y_i and the reflection coefficients Γ_i, and between Γ_i and the measured reflection coefficient ρ_i. Cross-ratio invariance implies that

$$\frac{\Delta_{m1}\Delta_{32}}{\Delta_{m2}\,\Delta_{13}} = \frac{(\rho_m - \rho_1)(\rho_3 - \rho_2)}{(\rho_m - \rho_2)(\rho_1 - \rho_3)} = \frac{(y_m - y_1)(y_3 - y_2)}{(y_m - y_2)(y_1 - y_3)} \quad (8)$$

which is formally equivalent to eqn. 7. Clearly, this idea can be extended to further bilinear transformations of ρ_i and y_i. From a practical point of view, it means that absolute values of the phase or magnitudes of the reflection coefficient are not required; we need only be concerned about drift and repeatability in the measurement system.

7.1 Admittance model I

We now consider the first of two equivalent circuit models for the probe. Cross-ratio invariance implies that the admittance of the probe can also undergo arbitrary bilinear transformation, without changing the form of eqn. 8. Applying the simple linear transformation

$$y'(\omega, \varepsilon_r) = \left(\frac{1}{j\omega C_0 Z_0}\right) \cdot y(\omega, \varepsilon_r) - \left(\frac{C_f}{C_0}\right) \quad (9)$$

to eqn. 4, we obtain

$$y'(\omega, \varepsilon_r) = \varepsilon_r + G_n \varepsilon_r^{5/2} \quad (10)$$

where $G_n = G_0/j\omega C_0$. Because of cross-ratio invariance, this linearly transformed admittance satisfies

$$\frac{(\rho_m - \rho_1)(\rho_3 - \rho_2)}{(\rho_m - \rho_2)(\rho_1 - \rho_3)} = \frac{(y'_m - y'_1)(y'_3 - y'_2)}{(y'_m - y'_2)(y'_1 - y'_3)} \quad (11)$$

To find the measured permittivity ε_m, eqn. 11 can be rewritten as a fifth-order polynomial in $\varepsilon_m^{1/2}$:

$$G_n \varepsilon_m^{5/2} + \varepsilon_m + \left[\frac{\Delta_{m1}\Delta_{32}\,y'_3\,y'_2 + \Delta_{m2}\,\Delta_{13}\,y'_1 y'_3 + \Delta_{m3}\,\Delta_{21} y'_2\,y'_1}{\Delta_{m1}\Delta_{32}\,y'_1 + \Delta_{m2}\,\Delta_{13}\,y'_2 + \Delta_{m3}\,\Delta_{21} y'_3}\right] = 0 \quad (12)$$

The coefficients of this polynomial are functions of the permittivities of the standard liquids $\{\varepsilon_1, \varepsilon_2, \varepsilon_3\}$ and the corresponding reflection-coefficient measurements $\{\rho_1, \rho_2, \rho_3\}$, the reflection coefficient ρ_m and the normalised radiation conductance G_n. This is a useful result; it means that the absolute values of G_0, C_f and C_0 need not, indeed *cannot*, be found using this calibration procedure. It follows that the set of corrected reflection coefficients $\{\Gamma_1, \Gamma_2, \Gamma_3\}$ cannot be calculated without knowledge of these equivalent circuit components.

The remaining problem is that G_n must be determined so that ε_m can be calculated from the measurement ρ_m. This is accomplished by measuring the probe reflection coefficient ρ_4 for another known dielectric with permittivity ε_4, setting $m = 4$ into eqn. 12, and solving the resulting quadratic in G_n. Once G_n is known, the permittivity of subsequently measured materials can be obtained from eqn. 12, which can be solved numerically for ε_m.

7.2 Short-circuit simplification

There are several advantages in using a short circuit as a known termination. From a practical point of view, a short is easy to make for this geometry, and from a computational point of view, eqn. 12 becomes much simpler, and so we have used the short-circuit termination as a reference for all our experimental measurements, using the following reduced form for processing the results. With known termination 1 identified as a short circuit, as $y_1 \to \infty$, eqn. 12 becomes

$$G_n \varepsilon_m^{5/2} + \varepsilon_m + \left[\frac{\Delta_{m2}\,\Delta_{13}}{\Delta_{m1}\Delta_{32}}\,y'_3 + \frac{\Delta_{m3}\,\Delta_{21}}{\Delta_{m1}\Delta_{32}}\,y'_2\right] = 0 \quad (13)$$

A further advantage of the short-circuit termination is that given a fourth measurement ρ_4 of a known material with permittivity ε_4, G_n can be calculated directly by setting $m = 4$ in eqn. 13 yielding

$$G_n = -\frac{\Delta_{41}\Delta_{32}\,\varepsilon_4 + \Delta_{42}\,\Delta_{13}\,\varepsilon_3 + \Delta_{43}\,\Delta_{21}\varepsilon_2}{\Delta_{41}\Delta_{32}\,\varepsilon_4^{5/2} + \Delta_{42}\,\Delta_{13}\,\varepsilon_3^{5/2} + \Delta_{43}\,\Delta_{21}\,\varepsilon_2^{5/2}} \quad (14)$$

7.3 Admittance model II

Neglecting G_n in eqns. 10 and 13, we obtain

$$\varepsilon_m = -\frac{\Delta_{m2}\,\Delta_{13}}{\Delta_{m1}\Delta_{32}}\,\varepsilon_3 - \frac{\Delta_{m3}\,\Delta_{21}}{\Delta_{m1}\Delta_{32}}\,\varepsilon_2 \quad (15)$$

For efficient computation, this expression can be rearranged as a bilinear transform of ρ_m. Because G_n is generally small, the value of ε_m calculated from eqn. 15 can be used as the starting point for the numerical computation of the root of eqn. 13.

Using eqn. 15, the permittivity ε_m can be calculated directly from reflection-coefficient measurements, without any knowledge of the equivalent circuit components C_0 and C_f. Although the equation is simple in form (a bilinear transform), it still embodies the error correction procedure for an arbitrary two-port error network.

Note that eqns. 13 and 15 are more general than they might appear from this analysis. Because of cross-ratio invariance, these expressions allow the probe admittance to be an arbitrary bilinear function of the material permittivity. Also, since the calibration is carried out separately at each measurement frequency, the probe circuit parameters are not necessarily invariant with frequency. However, the inadequacies of the simple admittance models remain.

7.4 Magnitude and phase calibration

The ADC in our digital recorder samples the output voltage from the magnitude and phase detectors of the network analyser. The reflection coefficient ρ_m is calculated from the ADC output word using

$$20 \log_{10} |\rho_m| = M_a \cdot \mathrm{ADC}_M + M_b \quad (16.1)$$

$$\frac{180}{\pi} \cdot \arg(\rho_m) = P_a \cdot \mathrm{ADC}_P + P_b \quad (16.2)$$

where M_a, M_b, P_a, P_b are frequency-independent constants, and ADC_M and ADC_P are the sampled magnitude and phase values. Cross-ratio invariance means that M_b and P_b do not have to be known at all, but we must still find M_a and P_a.

It is possible to rely on the intrinsic network-analyser calibration, but in the absence of expensive precision microwave standards, greater accuracy can be achieved by determining these two parameters with a numerical optimisation algorithm [24]. The measured permittivity of a standard liquid is calculated using eqn. 15, and the values of M_a and P_a are varied so that the calculated permittivity has the minimum squared deviation from the known permittivity of that liquid. The optimisation is carried out over the low-frequency range where the measured reflection coefficient is near to unity and the results are most sensitive to the errors in M_a and P_a, e.g. 50 to 500 MHz. In practice, the corrections are less than 3% in M_a and 8% in P_a.

8 Choice of standard liquids

The procedure for de-embedding from the network characterised by **E** requires measurements of materials with known dielectric properties. As well as a short-circuit reference, we have used air and 100 mM saline, with the dielectric dispersion parameters given by Stogryn* [25]. For admittance model I, G_n must be determined at each frequency, and so a third reference material is required; we have used methanol or ethanediol with the dielectric dispersion parameters and uncertainties reported by Jordan *et al.* [27].

Kraszewski *et al.* [28] surveyed some of the dielectric measurements available on polar liquids and concluded that deionised water has the lowest uncertainty and was therefore a good standard liquid. Anderson *et al.* [19] calculated and measured the effective capacitance of the open-ended line immersed in water and suggested that only 6 mm of water would be required to approximate an infinite sample to within 1% error using a 6.4 mm diameter probe.

Experimentally, we found that for low-loss high-permittivity liquids, such as deionised water, there were significant resonances associated with the dimensions of the beaker containing the liquid. In principle, these can be reduced by employing a large volume of liquid; where this is impractical, the beaker can be immersed in a larger volume of lossy liquid (e.g. saline) which reduces the reflections at the beaker walls [29, 30]. However, the resonance problem is less severe with the standard liquids we have used because they are inherently lossy over the measured frequency range.

9 Uncertainty analysis for dielectric measurements

The uncertainty in the measured permittivity ε_m can be estimated from bounds on the instrumentation uncertainties and the uncertainty in the permittivity of the known dielectric liquids. Fixed magnitude and phase errors are removed by the de-embedding procedure; the remaining instrumentation uncertainties that are significant are drift, noise, repeatability and nonlinearity. An experimental assessment of the effects of drift suggests that this is not significant over a two-hour measurement period, and the averaging performed by the recorder provides sufficient system noise reduction for resolution to be limited by the 12-bit ADC. Repeatability is improved by not having to connect and disconnect microwave terminations during calibration.

For the purposes of the uncertainty analysis, four assumptions about the system are made at the outset:

a The linear admittance model of eqn. 5 for the probe is exact.

b The systematic errors in the network analyser and test set are adequately represented by a scattering matrix.

c The uncertainties in M_a and P_a can be neglected.

d The uncertainties δm_i and δp_i in the magnitude and phase of the reflection coefficients $i = 1, 2, 3, 4$, m are much smaller than their magnitudes, and are bounded such that $|\delta_{m_i}| \leqslant \Delta M$ and $|\delta p_i| \leqslant \Delta P$.

With these assumptions, when the measured permittivity is calculated using eqn. 15, the uncertainty $\delta\varepsilon_m$ in ε_m is given by

$$\delta\varepsilon_m = \frac{\partial\varepsilon_m}{\partial\rho_m}\delta\rho_m + \sum_{i=1}^{3}\frac{\partial\varepsilon_m}{\partial\rho_i}\delta\rho_i + \sum_{i=2}^{3}\frac{\partial\varepsilon_m}{\partial\varepsilon_i}\delta\varepsilon_i \qquad (17)$$

where the $\delta\rho_i$ are the uncertainties in each reflection-coefficient measurement, and the $\delta\varepsilon_i$ are the uncertainties in the standard liquids. Note that these uncertainties are both complex quantities, and need careful interpretation. The partial derivatives are obtained by straightforward differentiation of eqn. 15, however their algebraic form is not particularly illuminating. Instead, the worst-case RMS error in the real and imaginary parts of the measured permittivity is calculated from eqn. 17 by substituting the measured values of the reflection coefficients and the bounds on their uncertainties.

10 Results and discussion

Figs. 3 and 4 show the measured permittivity of methanol and ethanediol at 20°C, together with bounds calculated from the uncertainties in previous measurements

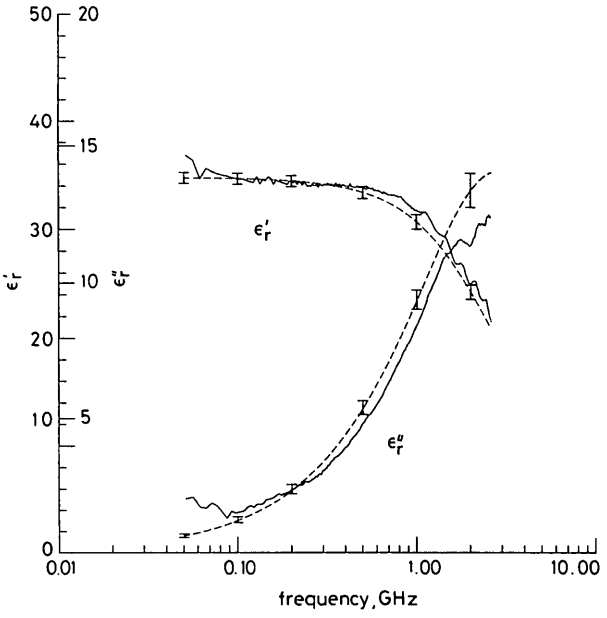

Fig. 3. *Measured permittivity of methanol at 20°C*
The permittivity was evaluated from the reflection-coefficient measurements using admittance model II. The graph also shows (broken line) the measurements reported by Jordan *et al.* [26], together with bounds calculated from their uncertainty estimates

reported by Jordan *et al.* [27]. These permittivities are calculated from the reflection-coefficient measurements with eqn. 15, using measurements of the probe in air ρ_2 and in 100 mM saline ρ_3 together with their corresponding permittivities ε_2 and ε_3. We emphasise that the permittivity is derived only from the *form* of the admittance

* Note that Malmberg and Maryott's equation for the static permittivity of water as reproduced by Stogryn has a typographical error. The correct version can be found on p. 145 of Grant *et al.* [26].

model of the open-ended probe, without needing the numerical values of the capacitances.

Fig. 5 shows the calculated bounds on the permittivity of ethanediol corresponding to assumed frequency-

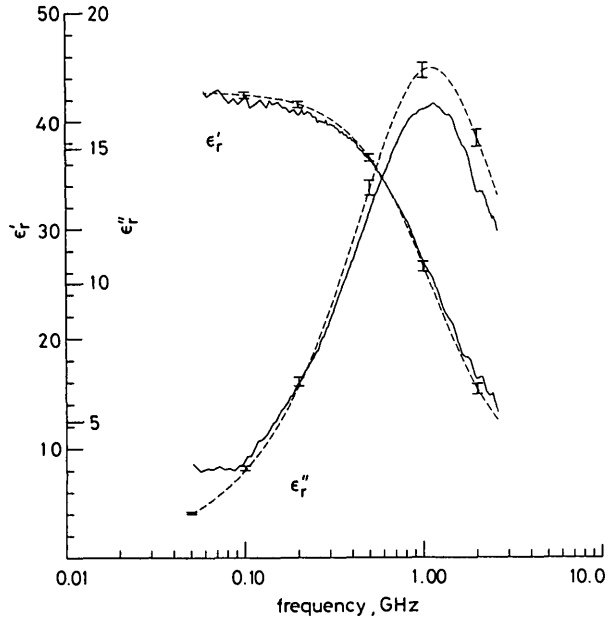

Fig. 4 *Measured permittivity of ethanediol at 20°C*

The permittivity was evaluated using admittance model II. The graph also shows (broken line) the measurements reported by Jordan *et al.* [26], together with bounds calculated from their uncertainty estimates

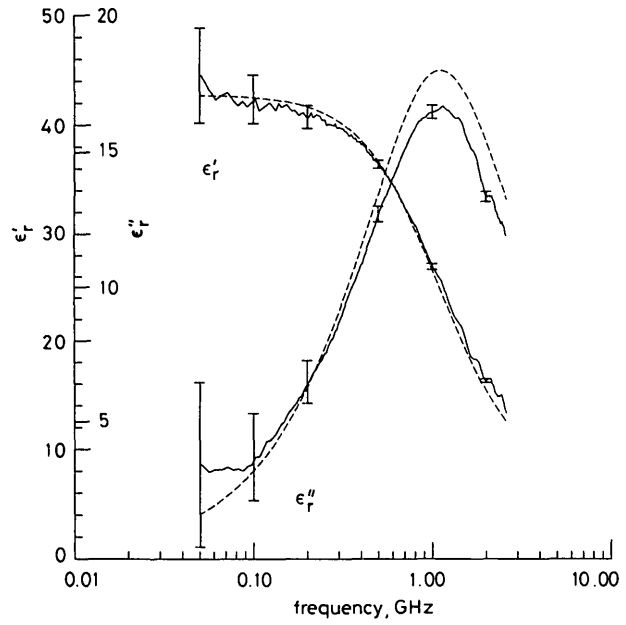

Fig. 5 *Measured permittivity of ethanediol at 20°C*

Shown together with calculated bounds on the measured permittivity corresponding to frequency-independent measurement uncertainties of 0.02 dB and 0.02°

independent uncertainties of 0.02 dB in magnitude and 0.2° in phase. These are calculated from the measured data using eqn. 17, with the $\delta\varepsilon_i$ set to zero, since uncertainty estimates are not available for the permittivity of 100 mM saline. Table 1 gives the magnitudes of the largest derivatives in eqn. 17 calculated at several frequencies which illustrates the change in error sensitivity with frequency changes.

At low frequencies (< 500 MHz), the probe is very sensitive to errors in magnitude and phase. Broadly speaking, the magnitude errors control the uncertainty in ε_r', and the phase errors control the uncertainty in ε_r''. For

Table 1: Magnitudes of derivatives in eqn. 17 calculated from experimental data of Fig. 4

f, GHz	$\left\|\frac{\partial\varepsilon_m}{\partial\rho_1}\right\|$	$\left\|\frac{\partial\varepsilon_m}{\partial\rho_2}\right\|$	$\left\|\frac{\partial\varepsilon_m}{\partial\rho_3}\right\|$	$\left\|\frac{\partial\varepsilon_m}{\partial\rho_m}\right\|$	$\left\|\frac{\partial\varepsilon_m}{\partial\varepsilon_2}\right\|$	$\left\|\frac{\partial\varepsilon_m}{\partial\varepsilon_3}\right\|$
0.05	5.7	790	140	800	0.97	0.13
0.1	4.2	370	130	400	0.90	0.23
0.2	4.2	160	110	210	0.76	0.35
0.5	6.1	48	57	97	0.56	0.44
1	10	32	39	71	0.64	0.39
2	14	20	28	46	0.78	0.26

example, for the data shown in Fig. 4 at 100 MHz, a perturbation of 0.02 dB in magnitude corresponds to a change $\Delta\varepsilon_r = (-0.008, 0.89)$ in permittivity, and a perturbation of 0.2° in phase corresponds to a change of $\Delta\varepsilon_r = (1.6, 0.013)$. At high frequencies (> 1 GHz), because of the ω^3 dependence of G_n, the errors are dominated by the errors implicit in admittance model II ($G_n = 0$). This is illustrated by the accuracy improvement that can be seen in Fig. 6 where the ethanediol data of Fig. 4 have been

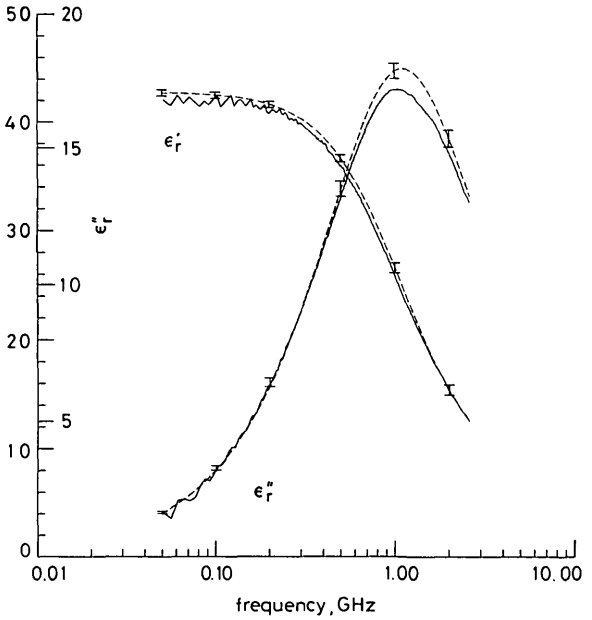

Fig. 6 *Measured permittivity of ethanediol at 20°C*

The permittivity was evaluated using admittance model I

recalculated using admittance model I eqn. 13. Here, G_n is calculated at each frequency from eqn. 14 using the methanol data of Fig. 3 as an additional standard ($G_n \simeq 10^{-4}$ at 1 GHz).

Fig. 7 shows the measured permittivity and effective conductivity of 150 mM saline at 20°C, calculated using admittance model II eqn. 15, together with the values predicted by the Stogryn formulas [25]. Also shown are the bounds on the permittivity and effective conductivity calculated from eqn. 17 assuming the same fixed instrumentation uncertainties errors as above. The effective conductivity is a more appropriate parameter for solutions which possess high DC conductivity and is calculated from $\omega\varepsilon_0\varepsilon_r''$. Fig. 8 shows the result of de-embedding the same data using admittance model I eqn. 13, with G_n calculated from methanol as before.

There is good agreement between the effective-conductivity results and those predicted by the Stogryn formula over the whole frequency range. This is not the case for the real part of the permittivity, which deviates significantly, particularly at low frequencies. It is difficult to identify the source of this deviation, although there is a

strong suggestion from Fig. 7 that this is dominated by systematic errors in the instrumentation. However, there is also the possibility that these errors may be due to

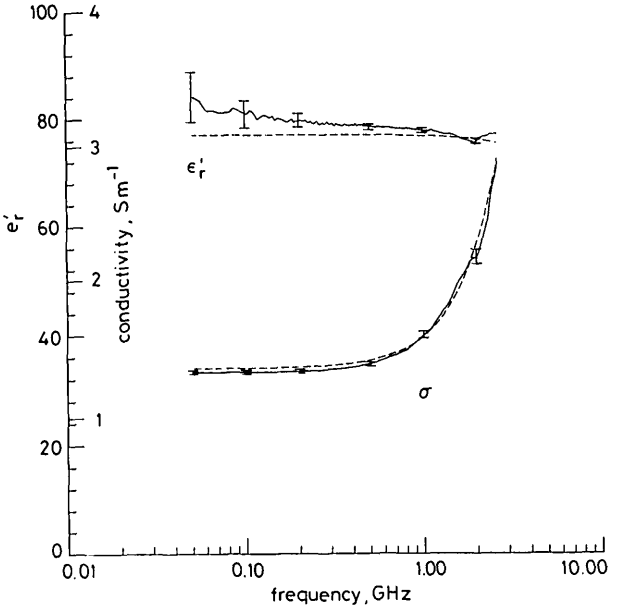

Fig. 7 *Measured permittivity and effective conductivity* $(=\omega\varepsilon_0\varepsilon''_r)$ *of 150 mM saline at 20°C*

Evaluated using admittance model II. The graph also shows the values predicted by the Stogryn formula [24]

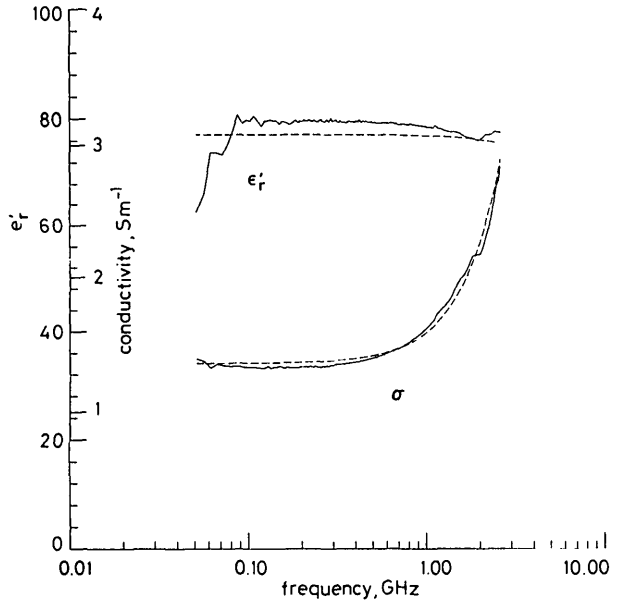

Fig. 8 *Measured permittivity and effective conductivity of 150 mM saline at 20°C*

Evaluated using admittance model I

permittivity-dependent variations in the probe capacitance. Grant *et al.* [30], following Mosig *et al.* [10], have shown that the capacitances and radiation conductance are, in general, functions of permittivity and frequency. Liping *et al.* [31] have derived a more complex admittance model, using radiation conductance terms involving higher powers of ε_r, which enables the probe to be used with greater accuracy at high frequencies. Both these approaches suggest that it might be possible to produce a more accurate expression for the probe admittance.

Note also the dip in the permittivity around 2 GHz, this is due to a resonance in the liquid in the beaker. This resonance effect is much larger in deionised water and largely precludes its use as a standard liquid, which is unfortunate since the dielectric properties of pure water are probably the most accurately known. A significant problem with using liquids as reference materials is the scarcity of accurate permittivity data in this frequency range.

Fig. 9 shows the measured permittivity of propan-1-ol at 20°C de-embedded with admittance model II, together

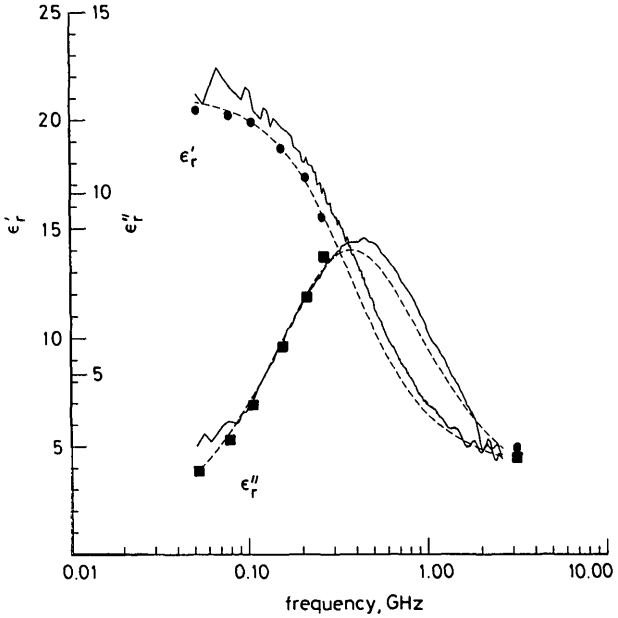

Fig. 9 *Measured permittivity of propan-1-ol at 20°C*

The original data obtained by Garg and Smyth [32] are plotted, together with a curve (broken line) derived by fitting their data to a three-component Debye dispersion

with the measured dielectric data of Garg and Smyth [32], giving good agreement over the frequency range investigated here.

For all the permittivity data on the standard liquids evaluated using the simpler admittance model II, the measured permittivities using the probe differ from previous dielectric measurements by less than 10%. This is acceptable for our application of the rapid rewarming of cryopreserved tissues and organs since we wish to assess only broad trends with changing temperature during the rewarming. Knowledge of the dielectric properties of perfusates and perfused tissue samples allows us to compute the power penetration depth and effective conductivity as a function of temperature. This information can be used to select a specific frequency at which rapid rewarming is best attempted, and is the fundamental basis for the design of an applicator for rewarming cryopreserved tissue. As an example of our measurements on materials relevant to organ cryopreservation, which are described in detail elsewhere [5], Fig. 10 shows the permittivity and effective conductivity of an experimental perfusate (3 mol/l glycerol in water, with 269 mmol/l of glucose) plotted over a range of temperatures.

11 Conclusions

We have described a complete dielectric measurement system for measuring the properties of liquids and biological tissues over a frequency range from 50 MHz to 2.6 GHz, using an open-ended probe as a sensor.

Dielectric liquids were used as known terminations for the probe, together with an approximate equivalent circuit for the probe input admittance. This scheme

allowed the permittivity to be calculated from the reflection coefficient in a particularly simple way, without needing absolute values of the fringing capacitances or radiation conductance.

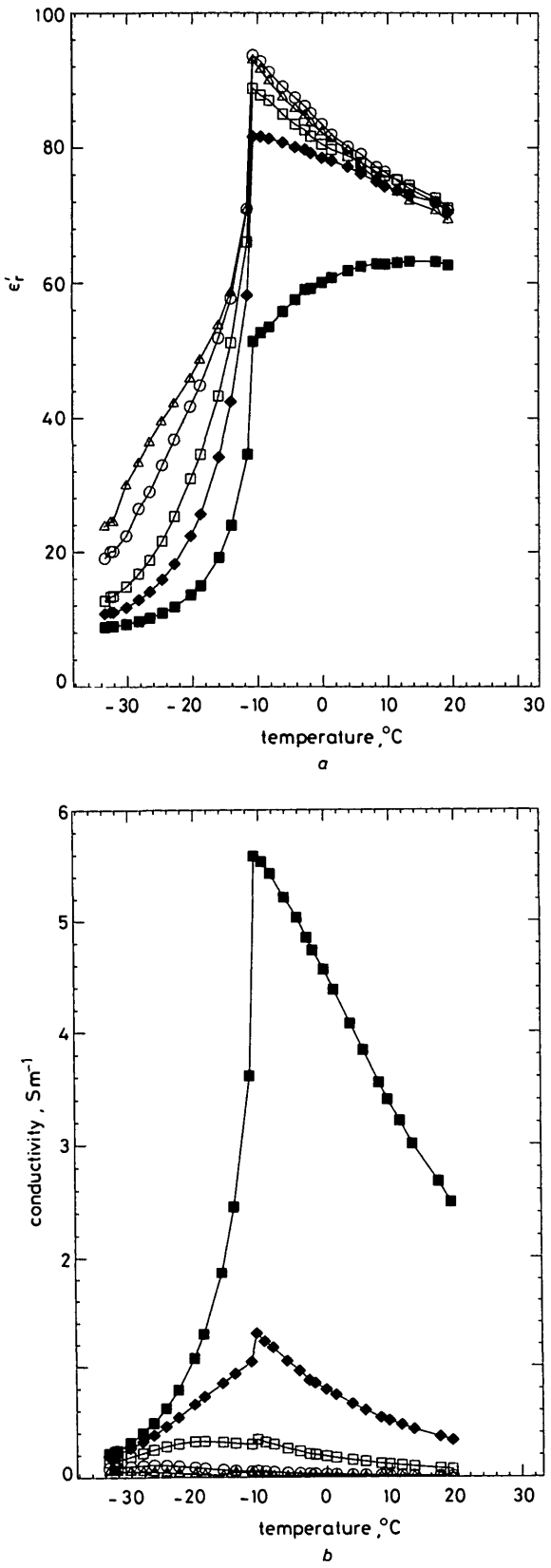

Fig. 10. *Permittivity and effective conductivity of an experimental perfusate with temperature*

a Measured permittivity
b Effective conductivity
3 *M* glycerol containing 269 m*M* glucose over −34 to +20°C. The permittivity and effective conductivity are plotted at five of the frequencies allocated for industrial, scientific and medical use: △ = 84 MHz; ○ = 168 MHz; □ = 434 MHz; ◆ = 896 MHz; ■ = 2.45 GHz

The accuracy of the measurements is restricted at low frequencies by the systematic errors in the network analyser, and at high frequencies by the inadequate circuit model for the probe. Nevertheless, the resulting system uncertainties are acceptable (better than 10%) for a survey of the dielectric properties of lossy materials over a range of frequencies and temperatures. The geometry of the open-ended probe sensor means that little or no sample preparation is required: this is a particular advantage with semisolid materials.

12 Acknowledgments

We would like to express our thanks to Dr. A.C. Metaxas and the Electricity Council for the loan of the network analyser and to M.P. Diaper for preparing the solutions used in this work.

13 References

1 METAXAS, A.C., and MEREDITH, R.J.: 'Industrial microwave heating' (Peter Peregrinus, London, 1983)
2 STROHBEHN, J.W., CETAS, T.C., and HAHN, G.M.: 'Guest editorial — Special Issue on Hyperthermia and cancer therapy', *IEEE Trans.*, 1984, **BME-31,** (1), p. 1
3 AFSAR, M.N., BIRCH, J.R., CLARKE, R.N., and CHANTRY, G.W. (ed.): 'The measurement of the properties of materials', *Proc. IEEE*, 1986, **74,** (1), pp. 183–199
4 BURDETTE, E.C., WIGGINS, S., BROWN, R., and KAROW, JR., A.M.: 'Microwave thawing of frozen kidneys: A theoretically based experimentally effective design', *Cryobiology*, 1980, **17,** pp. 393–402
5 MARSLAND, T.P., EVANS, S., and PEGG, D.E.: 'Dielectric measurements for the design of a rapid rewarming system', accepted for publication in *Cryobiology*, 1987, **24**
6 SMITH, G.S., and NORDGARD, J.D.: 'Measurement of the electrical constitutive parameters of materials using antennas', *IEEE Trans.*, 1985, **AP-33,** (7), pp. 783–792
7 TANABE, E., and JOINES, W.T.: 'A nondesctructive method for measuring the complex permittivity of dielectric materials at microwave frequencies using an open transmission line resonator', *IEEE Trans.*, 1976, **IM-25,** (3), pp. 222–226
8 BURDETTE, E.C., CAIN, F.L., and SEALS, J.: '*In vivo* probe measurement technique for determining dielectric properties at VHF through microwave frequencies', *IEEE Trans.*, 1980, **MTT-28,** (4), pp. 414–427
9 STUCHLY, M.A., and STUCHLY, S.S.: 'Permittivity of mammalian tissues *in vivo* and *in vitro*. Advances in experimental techniques and recent results', *Int. J. Electron.*, 1984, **56,** (4), pp. 443–456
10 MOSIG, J.R., BESSON, J-C.E., GEX-FABRY, M., and GARDIOL, F.E.: 'Reflection of an open-ended coaxial line and application to nondestructive measurement of materials', *IEEE Trans.*, 1981, **IM-30,** (1), pp. 46–51
11 DESCHAMPS, G.A.: 'Impedance of an antenna in a conducting medium', *IRE Trans.*, 1962, **AP-10,** (5), pp. 648–650
12 BRADY, M.M., SYMONS, S.A., and STUCHLY, S.S.: 'Dielectric behaviour of selected animal tissues *in vitro* at frequencies from 2 to 4 GHz', *IEEE Trans.*, 1981, **BME-28,** (3), pp. 305–307
13 MARCUVITZ, N.: 'The waveguide handbook' (MIT Radiation Laboratory & McGraw-Hill, 1951), pp. 213–216
14 BAHL, I.J., and STUCHLY, S.S.: 'Effect of finite size of ground plane on the impedance of a monopole immersed in a lossy medium', *Electron. Lett.*, 1979, **15,** (22), pp. 728–729
15 ATHEY, T.W., STUCHLY, M.A., and STUCHLY, S.S.: 'Measurement of radio frequency permittivity of biological tissues with an open-ended coaxial line: Part I', *IEEE Trans.*, 1982, **MTT-30,** (1), pp. 82–86
16 STUCHLY, M.A., ATHEY, T.W., SAMARAS, G.M., and TAYLOR, G.E.: 'Measurement of radio frequency permittivity of biological tissues with an open-ended coaxial line: Part II', *ibid.*, 1982, **MTT-30,** (1), pp. 87–92
17 TRAN, V.N., STUCHLY, S.S., and KRASZEWSKI, A.: 'Dielectric properties of selected vegetables and fruits 0.1–10.0 GHz', *J. Microwave Power*, 1984, **19,** (4), pp. 251–258
18 STUCHLY, M.A., BRADY, M.M., STUCHLY, S.S., and GAJDA, G.: 'Equivalent circuit of an open-ended coaxial line in a lossy dielectric', *IEEE Trans.*, 1982, **IM-31,** (2), pp. 116–119

19 ANDERSON, L.S., GAJDA, G.B., and STUCHLY, S.S.: 'Analysis of an open-ended coaxial line sensor in layered dielectrics', *ibid.*, 1986, **IM-35,** (1), pp. 13–18
20 MARSLAND, T.P.: 'Dielectric measurements for organ cryopreservation'. PhD thesis, University of Cambridge, UK, Jan. 1986
21 KRASZEWSKI, A., STUCHLY, M.A., and STUCHLY, S.S.: 'ANA calibration method for measurements of dielectric properties', *IEEE Trans.*, 1983, **IM-32,** (2), pp. 385–387
22 BIANCO, B., and PARODI, M.: 'Measurement of the effective relative permittivities of microstrip', *Electron. Lett.*, 1975, **11,** (3), pp. 71–72
23 KREYSZIG, E.: 'Advanced engineering mathematics' (John Wiley & Sons, New York, 1979), 4th Edn., pp. 613–614
24 'E04JBF routine document', *in* 'NAG Fortran library Mk. 6' (The Numerical Algorithms Group, 1977)
25 STOGRYN, A.: 'Equations for calculating the dielectric constant of saline water', *IEEE Trans.*, 1971, **MTT-19,** pp. 733–736
26 GRANT, E.H., SHEPPARD, R.J., and SOUTH, G.P.: 'Dielectric behaviour of biological molecules in solution' (Clarendon Press, Oxford, 1978)
27 JORDAN, B.P., SHEPPARD, R.J., and SZWARNOWSKI, S.: 'The dielectric properties of formamide, ethanediol and methanol', *J. Phys. D*, 1978, **11,** pp. 695–701
28 KRASZEWSKI, A., STUCHLY, S.S., STUCHLY, M.A., and SYMONS, S.A.: 'On the measurement accuracy of the tissue permittivity *in vivo*', *IEEE Trans.*, 1983, **IM-32,** (1), pp. 37–42
29 KING, R.W.P., and SMITH, G.S.: 'Antennas in matter' (MIT Press, Cambridge, MA, USA, 1981), pp. 755–765
30 GRANT, J.P., CLARKE, R.N., SYMM, G.T., and SPYROU, N.M.: 'A critical study of the open-ended coaxial line sensor for medical and industrial dielectric measurements'. IEE Colloquium on Industrial and Medical Applications of Microwaves, IEE Colloquium Digest, 1986/73
31 LIPING, L., DEMING, X., and ZHIYAN, J.: 'Improvement in dielectric measurement technique of open-ended coaxial line resonator method', *Electron. Lett.*, 1986, **22,** (7), pp. 373–375
32 GARG, S.K., and SMYTH, C.P.: 'Microwave absorption and molecular structure in liquids. LXII. The three dielectric dispersion regions of the normal primary alcohols.' *J. Phys. Chem.*, 1965, **69,** (4), pp. 1294–1301